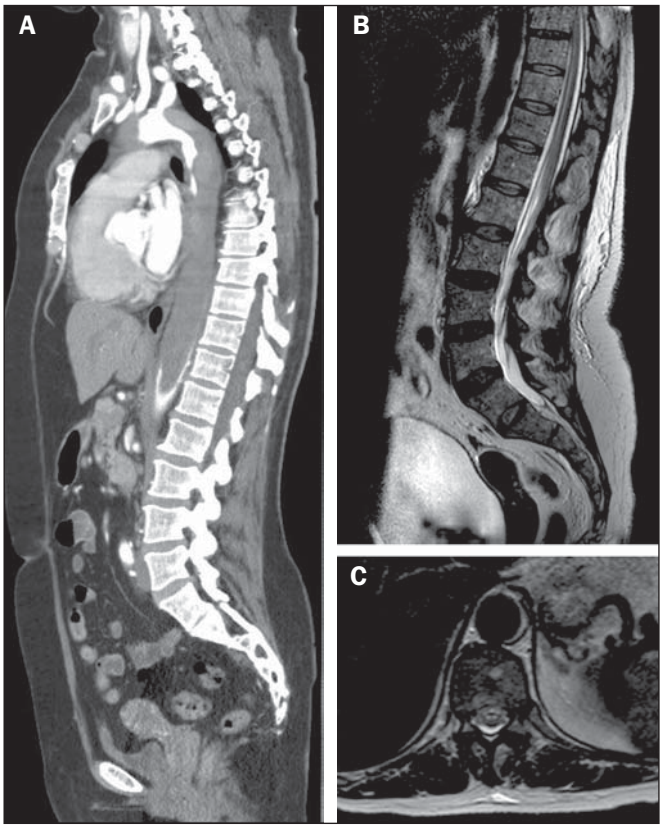

Figure 1. A: Maximum intensity projection reconstruction of computed tomography angiography in the sagittal plane showing an extensive mural thrombus in the thoracic aorta, extending to the infrarenal aorta. **B:** Sagittal T2-weighted MRI sequence showing areas of hyperintensity within the anterior spinal cord. **C:** Axial T2-weighted MRI at the level of the T10 spinal segment demonstrating anterior areas of hyperintensity, with the "owl eye" sign.

diffusion of water at the levels studied. Cranial MRI revealed acute lesions (also with restricted diffusion) in the right middle cerebral artery. The patient underwent surgery to treat the aortic dissection, and her neurological function was monitored.

The evaluation of the aorta by imaging methods has been the subject of a series of recent publications in the Brazilian radiology literature[2–4]. In the case presented here, neurological findings were associated with aortic dissection, and the MRI findings were consistent with the diagnosis of spinal cord infarction with ischemic stroke in the right middle cerebral artery. Although spinal cord infarction is not a rare event[5], the subtlety of the findings and the wide range of differential diagnoses can make its diagnosis difficult. Spinal cord ischemia can be attributed to several causes, including aortic dissection (as in the case presented) and thoracolumbar sympathectomy, or can even occur as a postpartum complication. The single anastomotic segment that irrigates the anterior two thirds of the spinal cord (mainly by the artery of Adamkiewicz) is more susceptible to ischemia than is the posterior segment, which has several levels of vascular supply[6]. A high degree of clinical suspicion of neurological involvement of the spinal cord is indicative of the diagnosis. Symptoms vary depending on the extent of the affected area and the level of spinal injury. Cerebral ischemic lesion is also a possible complication of aortic dissection and can result from reduced blood flow to the brain caused by the surgical procedure or even from carotid involvement caused by dissection or embolism from the thrombus in the aorta. In addition, data in the literature indicate that there is a right-side dominance of lesions, which is explained by different mechanical dynamics in the progression of the dissecting hematoma.

MRI is particularly sensitive in the detection of aortic dissection and can reveal signal abnormality in the anterior horns of the spinal cord, which can be associated with enhancement after contrast agent injection. The spinal segment most often affected is the thoracic segment, due to the border arterial supply[6]. Diffusion sequences can show restriction in the ischemic area. In fact, diffusion sequences can provide early detection[7], although this technique is not always applied in routine MRI scans of the spinal cord. Therefore, we have presented a case of aortic dissection with a rare combination of neurological complications of brain and spinal cord ischemia.

REFERENCES

1. Udiya AK, Shetty GS, Singh V, et al. "Owl eye sign": anterior spinal artery syndrome. Neurol India. 2015;63:459.
2. Amaral RH, Souza VV, Nin CS, et al. Aortic lesion simulating pulmonary disease: a case report. Radiol Bras. 2014;47:320–2.
3. Metzger PB, Novero ER, Rossi FH, et al. Evaluation of preoperative computed tomography angiography in association with conventional angiography versus computed tomography angiography only, in the endovascular treatment of aortic diseases. Radiol Bras. 2013;46:265–72.
4. Netto OS, Hasselmann CL, Osterne ECV, et al. Detection of abdominal aortic calcification by densitometry. Radiol Bras. 2013;46:35–8.
5. Moulakakis KG, Mylonas SN, Dalainas I, et al. Management of complicated and uncomplicated acute type B dissection. A systematic review and meta-analysis. Ann Cardiothorac Surg. 2014;3:234–46.
6. Lee SJ, Kim JH, Na CY, et al. Eleven years of experience with the neurologic complications in Korean patients with acute aortic dissection: a retrospective study. BMC Neurol. 2013;13:46.
7. Fujikawa A, Tsuchiya K, Takeuchi S, et al. Diffusion-weighted MR imaging in acute spinal cord ischemia. Eur Radiol. 2004;14:2076–8.

Igor Aloísio Garcez Zamilute[1], Fabiano Reis[1], Nivaldo Adolfo Silva Junior[1], Tania Aparecida Marchiori de Oliveira Cardoso[1], Wendy Caroline de Souza Costa França[1]

1. Faculdade de Ciências Médicas da Universidade Estadual de Campinas (FCM-Unicamp), Campinas, SP, Brazil. Mailing address: Dr. Igor Aloísio Garcez Zamilute. Faculdade de Ciências Médicas, Departamento de Radiologia, Unicamp. Rua Tessália Vieira de Camargo, 126, Cidade Universitária Zeferino Vaz. Campinas, SP, Brazil, 13083-887. E-mail: zamilute1@hotmail.com.

http://dx.doi.org/10.1590/0100-3984.2015.0070

Use of multislice computed tomography in the diagnosis of annular constrictive pericarditis

Dear Editor,

A 65-year-old man with a history of pleural tuberculosis was referred to our outpatient clinic due to respiratory difficulty. He presented with worsening dyspnea on minimal exertion. Examination confirmed that the patient was experiencing mild respiratory difficulty; his respiration rate was 25 breaths per minute, and his heart rate was 98 beats per minute. Cyanosis, jaundice, and signs of heart failure were absent, and other systems appeared normal. Multislice computed tomography showed a calcified pericardial band encircling the left ventricular cavity at the level of the atrioventricular groove (Figure 1).

Complete pericardiectomy was performed successfully and the postoperative course was uneventful. Histopathologic examination of the excised pericardium showed fibrocollagenous thickening with areas of hemorrhage and heavy calcific deposits. No areas of granuloma or vasculitis were identified. The final diagnosis was annular constrictive pericarditis.

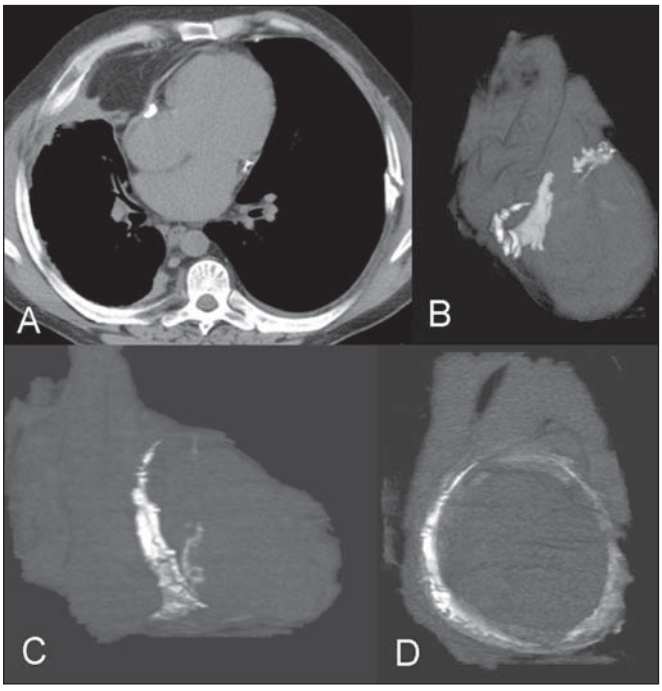

Figure 1. Axial computed tomography image (**A**) and volume-rendered reconstructions (**B–D**) showing a calcified pericardial band encircling the left ventricular cavity at the level of the atrioventricular groove.

Constrictive pericarditis is characterized by thick pericardial fibrosis and frequent calcification that progressively impairs diastolic filling of the heart, with associated symptoms of heart failure[1]. Annular constrictive pericarditis is extremely rare, and few similar cases have been reported[1]. Previous pericardiectomy, congenital heart disease, and complications of tuberculosis may be the leading causes of this condition. Depending on the location of the pericardial constriction, the clinical presentation of localized constriction may differ, including obstruction of the right ventricular outflow tract, coronary obstruction, and pulmonary stenosis[1–3]. The imaging evaluation of cardiovascular calcifications has been the subject of a series of recent publications in the Brazilian radiology literature[4–7]. Multislice computed tomography may be an important tool for the precise identification of annular constrictive pericarditis[8].

REFERENCES

1. Butany J, El Demellawy D, Collins MJ, et al. Constrictive pericarditis: case presentation and review of the literature. Can J Cardiol. 2004;20: 1137–44.
2. Nigri A, Mangieri E, Martuscelli E, et al. Pulmonary trunk stenosis due to constriction by a pericardial band. Am Heart J. 1987;114:448–50.
3. Mounsey P. Annular constrictive pericarditis. With an account of a patient with functional pulmonary, mitral, and aortic stenosis. Br Heart J. 1959;21:325–34.
4. Barbosa JHO, Santos AC, Salmon CEG. Susceptibility weighted imaging: differentiating between calcification and hemosiderin. Radiol Bras. 2015;48:93–100.
5. Neves PO, Andrade J, Monção H. Coronary anomalies: what the radiologist should know. Radiol Bras. 2015;48:233–41.
6. Araújo Neto CA, Oliveira Andrade AC, Badaró R. Intima-media complex in the investigation of atherosclerosis in HIV-infected patients [Letter to the Editor]. Radiol Bras. 2014;47(1):x.
7. Brasileiro Junior VL, Luna AHB, Sales MAO, et al. Reliability of digital panoramic radiography in the diagnosis of carotid artery calcifications. Radiol Bras. 2014;47:28–32.
8. Matsuno Y, Shimabukuro K, Ishida N, et al. Off-pump complete pericardiectomy for an unusual case of annular constrictive pericarditis. Ann Thorac Surg. 2012;94:e45–7.

Bruno Hochhegger[1], Klaus L. Irion[2], Gláucia Zanetti[3], Edson Marchiori[3]

1. Universidade Federal de Ciências da Saúde de Porto Alegre (UFCSPA), Porto Alegre, RS, Brazil. 2. Liverpool Heart and Chest Hospital – NHS Trust, Liverpool, United Kingdom. 3. Universidade Federal do Rio de Janeiro (UFRJ), Rio de Janeiro, RJ, Brazil. Mailing address: Dr. Edson Marchiori. Rua Thomaz Cameron, 438, Valparaíso. Petrópolis, RJ, Brazil, 25685-120. E-mail: edmarchiori@gmail.com.

http://dx.doi.org/10.1590/0100-3984.2015.0151

Post-Oberlin procedure cortical neuroplasticity in traumatic injury of the upper brachial plexus

Dear Editor,

A 27-year-old left-handed male injured his left arm in a motorcycle accident. The clinical examination showed a lack of movement in the left forearm and shoulder, with normal movement of the left hand. Magnetic resonance imaging (MRI) showed avulsion of left upper nerve roots (C5 and C6) of the brachial plexus, caused by traumatic lesion. He underwent neurotization by the Oberlin procedure and transfer of the accessory nerve to the suprascapular nerve three months after the accident[1]. The first signs of re-innervation of the biceps muscle appeared two months after the surgical procedure. The patient later showed significant signs of recovery.

We selected this patient to undergo functional MRI (fMRI). For the fMRI acquisition, we also selected one healthy control volunteer who was matched to the patient for age, gender, and handedness. Both subjects underwent MRI in order to compose a structural sequence with anatomical images. In the functional sequence, we employed the following acquisition parameters: repetition time = 2000 ms; echo time = 30 ms; flip angle = 90°; matrix = 64 × 64; field of view = 240 mm; voxel resolution = 3.75 × 3.75 × 5 mm; slice thickness = 5 mm; sagittal plane, 22 planes.

The motor tasks consisted of elbow flexion and hand grasping, in a "block" design: hand grasping of the dominant injured limb (left upper limb) and elbow flexion of the injured and healthy limbs. All motor tasks were alternated with a rest period (there were 100 dynamics per block, and there were 10 rest dynamics for each set of 10 task dynamics). Ten blocks of each state (resting and limb movement) were used. The patient and the healthy volunteer performed the same tasks. The MRI of the patient showed no anatomical alterations. After family-wise error correction at a value of $p < 0.05$, all fMRI scans acquired during the motor tasks showed main activation of the contralateral hemisphere in the areas that correspond to the primary motor cortex (Figure 1), as follows: forearm and hand for hand grasping of the left upper limb; arm, forearm, hand, and face for left elbow flexion; arm and forearm for flexion of the right upper limb. The MRI of the healthy volunteer also showed no anatomical alterations.

In the case reported here, fMRI was effective in identifying the cortical activations. The comparison between the patient and the healthy volunteer showed that the areas of cortical activation were quite similar, as were the activation peaks. The detectable reactivation of the cortical area in the patient during flexion of the injured elbow corresponded to the arm area in the motor homunculus of the volunteer[2–8]. The cortical activations in this case were similar to those reported in previous studies that applied